Jeremy D. Eekhoff
Department of Biomedical Engineering,
Washington University in St. Louis
One Brookings Drive,
St. Louis, MO 63130

Fei Fang
Department of Mechanical Engineering
and Materials Science,
Washington University in St. Louis,
One Brookings Drive,
St. Louis, MO 63130

Lindsey G. Kahan
Department of Biomedical Engineering,
Washington University in St. Louis,
One Brookings Drive,
St. Louis, MO 63130

Gabriela Espinosa
Department of Biomedical Engineering,
Washington University in St. Louis,
One Brookings Drive,
St. Louis, MO 63130

Austin J. Cocciolone
Department of Biomedical Engineering,
Washington University in St. Louis,
One Brookings Drive,
St. Louis, MO 63130

Jessica E. Wagenseil
Department of Mechanical Engineering and
Materials Science,
Washington University in St. Louis,
One Brookings Drive,
St. Louis, MO 63130

Robert P. Mecham
Department of Cell Biology and Physiology,
Washington University in St. Louis,
660 South Euclid Avenue,
St. Louis, MO 63110

Spencer P. Lake[1]
Department of Mechanical Engineering and
Materials Science,
Washington University in St. Louis,
One Brookings Drive,
St. Louis, MO 63130;
Department of Biomedical Engineering,
Washington University in St. Louis,
One Brookings Drive,
St. Louis, MO 63130;
Department of Orthopaedic Surgery,
Washington University in St. Louis,
One Brookings Drive,
St. Louis, MO 63130
e-mail: lake.s@wustl.edu

Functionally Distinct Tendons From Elastin Haploinsufficient Mice Exhibit Mild Stiffening and Tendon-Specific Structural Alteration

Elastic fibers are present in low quantities in tendon, where they are located both within fascicles near tenocytes and more broadly in the interfascicular matrix (IFM). While elastic fibers have long been known to be significant in the mechanics of elastin-rich tissue (i.e., vasculature, skin, lungs), recent studies have suggested a mechanical role for elastic fibers in tendons that is dependent on specific tendon function. However, the exact contribution of elastin to properties of different types of tendons (e.g., positional, energy-storing) remains unknown. Therefore, this study purposed to evaluate the role of elastin in the mechanical properties and collagen alignment of functionally distinct supraspinatus tendons (SSTs) and Achilles tendons (ATs) from elastin haploinsufficient (HET) and wild type (WT) mice. Despite the significant decrease in elastin in HET tendons, a slight increase in linear stiffness of both tendons was the only significant mechanical effect of elastin haploinsufficiency. Additionally, there were significant changes in collagen nanostructure and subtle alteration to collagen alignment in the AT but not the SST. Hence, elastin may play only a minor role in tendon mechanical properties. Alternatively, larger changes to tendon mechanics may have been mitigated by developmental compensation of HET tendons and/or the role of elastic fibers may be less prominent in smaller mouse tendons compared to the larger bovine and human tendons evaluated in previous studies. Further research will be necessary to fully elucidate the influence of various elastic fiber components on structure–function relationships in functionally distinct tendons.
[DOI: 10.1115/1.4037932]

Introduction

Tendon exhibits a highly hierarchical structure, being composed of collagen bundles of increasing size from fibrils to fibers to fascicles to whole tendon [1,2]. These bundles are generally aligned with the long axis of the tendon, yet can form local substructures such as helices and braids [1,3]. The complex hierarchical structure of tendons allows for transmission of forces across multiple length scales, which is evidenced by fiber sliding and reorientation upon application of a mechanical load [4,5]. This characteristic reorganization, along with fiber uncrimping, is thought to dominate the low strain response of tendon before the fibers fully engage [6–8].

[1]Corresponding author.
Manuscript received August 14, 2017; final manuscript received September 11, 2017; published online September 27, 2017. Assoc. Editor: Kyle Allen.

Many studies have focused on the role of collagen in tendon mechanics due to its primacy in tendon structure and composition, yet recent studies have also begun to investigate how noncollagenous components affect tendon function [9]. One potential contributor to tendon mechanics is elastic fibers, which are composed of a core of elastin surrounded by a scaffold of fibrillin-based microfibrils [10,11]. Elastic fibers are formed primarily during development and remain intact throughout the majority of the lifetime of the organism [12]; yet still, elastic fiber degradation is common in advanced age and may contribute to decreased fatigue resistance in tendon [13,14]. Furthermore, a number of human genetic diseases including cutis laxa, Marfan syndrome, and Weill–Marchesani syndrome are associated with abnormal elastic fiber formation and atypical joint laxity [10,15,16]. In addition, a relationship between chronic tendinopathy and loss of elastic fibers has been reported in tendon [17,18]. Finally, elastin and fibrillin-1 are upregulated in torn tendons, suggesting that elastic fibers may be involved in the healing process [19].

Elastic fibers can endow unique mechanical properties to tissues. Isolated elastin is highly extensible, elastic, and resilient, and therefore, is capable of withstanding up to 100% strain without permanent deformation or large energy loss upon unloading [20,21]. Consequently, elastic fibers are abundant in tissue where elasticity and resiliency are required, such as arterial vasculature, skin, and the lungs. However, elastic fibers account for only 1–2% of the dry weight of tendon [1], where they have been shown to be located along rows of tenocytes within fascicles and more broadly between fascicles in the interfascicular matrix (IFM) [22,23]. Despite this small proportion of elastic fibers, recent studies have suggested that the fibers significantly influence the mechanics of tendons and ligaments in tension and shear [24–27], conceivably by maintaining collagen crimp and facilitating sliding between fascicles.

The aforementioned studies investigating elastic fibers in connective tissue have used elastase to selectively digest elastin. However, elastase treatment may have off-target effects that could confound the results of those experiments. Alternatively, while elastin knockout mice ($Eln^{-/-}$) die perinatally from obstructive arterial disease [28], elastin haploinsufficient mice ($Eln^{+/-}$, HET) exhibit ~50% of normal elastin expression, possess altered arterial morphology and mechanical properties, yet still maintain normal gross appearance and activity [29–31]. This study utilized elastin haploinsufficient mice as a unique tool to quantify the effects of decreased elastin on the mechanics of the supraspinatus tendon (SST) and Achilles tendon (AT).

Coordinated evaluation of these functionally distinct tendons is critical, because it has been shown that there are differences in elastic fiber content and corresponding mechanical properties between the positional common digital extensor tendon and the energy-storing superficial digital flexor tendon in horses, suggesting that the role of elastic fibers in tendon mechanics is likely more prominent in energy-storing tendons [14,32,33]. In mice, the SST experiences multiaxial loading in vivo and is one of the four tendons in the rotator cuff which maintain positioning of the shoulder joint, while the AT experiences larger strains in vivo and stores and releases energy to reduce the energy cost of locomotion, similar to the equine superficial digital flexor tendon [34]. Therefore, we hypothesized that the elastin deficient tendons would have impaired low strain response in tension, and that the effect of elastin deficiency would be greater in the energy-storing AT than in the positional SST.

Methods

Sample Preparation. Male $Eln^{+/+}$ (wild type, WT) and $Eln^{+/-}$ (HET) mice between 3 and 4 months of age were euthanized by CO_2 asphyxiation and frozen at −20° C until use. On the day of dissection, mice were thawed at 4 °C for approximately 6 h. Left and right humeral head-SST and calcaneus-AT complexes were removed from each mouse using a stereo microscope (Olympus, SZ2-ILST, Tokyo, Japan) to aid in visualization to ensure proper removal of muscle and other surrounding tissues. After dissection, the samples were stored at 4 °C in phosphate-buffered saline soaked gauze for no longer than 15 h before use. All animal procedures were approved by the Institutional Animal Care and Use Committee.

Biochemical Analysis. Elastin, collagen, and total protein levels were determined using amino acid based biochemical assays ($n = 6$ per group). Tendons were hydrolyzed with 6 N HCl at 110 °C for 48 h. A competitive enzyme-linked immunosorbent assay (ELISA) was performed to determine elastin content using an antibody raised against desmosine [35]. Briefly, an ELISA plate coated with a desmosine-ovalbumin conjugate (Elastin Products Company, DOC375, Owensville, MO) was blocked before adding the sample and desmosine antibody (provided by Barry Starcher, University of Texas Health Science Center). Peroxidase-labeled antirabbit IgG (KPL, 074-1506, Milford, MA) was used as the secondary antibody. Absorbance at 650 nm was measured 20 min after the addition of a peroxidase substrate (KPL, 5120-0081, Milford, MA). The elastin content was determined by comparing the absorbance to a standard curve generated using hydrolyzed elastin (Elastin Products Company, E60, Owensville, MO). Hydroxyproline levels were determined with a Chloramine T assay, using a hydroxyproline standard (Sigma-Aldrich, H54409, St. Louis, MO) and measuring absorbance at 550 nm [36]. Collagen levels were calculated assuming that the collagen is composed of 13.5% hydroxyproline by mass [37]. Both elastin and collagen content were normalized by total protein, which was determined with a ninhydrin assay using an amino acid calibrator (Pickering Labs, 012506C, Mountain View, CA) and absorbance measured at 575 nm [38].

Two-Photon Microscopy. Elastin distribution in tendons was visualized using fluorescent imaging with sulforhodamine B (SRB), which has been shown to fluorescently stain elastic fibers with higher intensity than collagen fibers [25,39]. Intact SSTs and ATs ($n = 6$ for each genotype) were incubated in 0.5 mg/ml SRB solution for 1 min and in 1 μg/ml DAPI solution for 5 min to stain nuclei. The Mai Tai broadband infrared multiphoton laser of a multiphoton confocal microscope system (Zeiss, LSM 880, Oberkochen, Germany) was set to 800 nm excitation, and signals from elastic fibers and nuclei were collected at 565–600 nm and 450–490 nm, respectively. Digital images were obtained in the midsubstance of the tendons for qualitative analysis.

Transmission Electron Microscopy. In addition to the SRB stained images, transmission electron microscopy (TEM) micrographs were obtained to examine the elastic fibers and collagen structure on the nanoscale. Samples of intact tendon ($n = 3$–4 per group) were aldehyde fixed and embedded in araldite resin. Ultrathin transverse sections were cut from the midsubstance of the tendon and stained with 1% uranyl acetate and Reynold's lead citrate. Multiple images were acquired throughout the sections using a TEM (JEOL, JEM-1400, Tokyo, Japan) at 25,000× magnification. Subsequently, the images were analyzed using IMAGEJ software to quantify individual collagen fibril diameters (minor diameter of best fit ellipse) and collagen area fraction [40]. The number of images analyzed was such that a minimum of 1000 total fibrils were analyzed for each sample.

Biomechanical Testing. The humeral head-SST (WT $n = 13$; HET $n = 10$) and calcaneus-AT (WT $n = 8$; HET $n = 11$) complexes were scanned using a laser scanning device (Keyence, LJ-V7080, Osaka, Japan) and a custom MATLAB code was used to calculate the average cross-sectional area (CSA) of the tendon midsubstance. The samples were then clamped in a custom

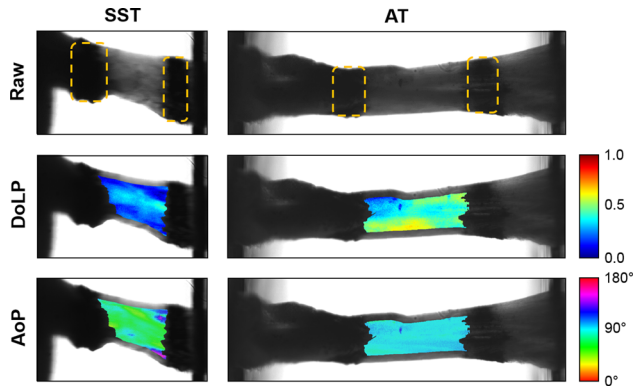

Fig. 1 Images of a representative SST and AT prior to ramp to failure taken using the QPLI system. The bone is fixed on the left, and the free end of the tendon is clamped on the right. Stain lines, outlined with dotted lines, mark the boundaries of the ROI for analysis of DoLP and AoP. Data are analyzed as groups of pixels, where the AVG DoLP and STD AoP represent the strength of alignment and uniformity of orientation, respectively.

aluminum fixture with the free end of the tendon secured between two pieces of sandpaper. Two lines were applied perpendicular to the long axis of the tendon using Verhoeff's stain to optically track strain and define a region of interest (ROI) for collagen alignment analysis (described below). The fixture was secured to actuators of a linear mechanical testing machine (TestResources, 574LE2, Shakopee, MN) with the tendon submerged in a phosphate-buffered saline bath to maintain hydration. After applying a 0.1 N preload to remove any slack present in the tendon, the distance between the clamps was measured and recorded as the initial gauge length. The sample was subjected to preconditioning, stress relaxation, and ramp to failure. Specific details of the test protocol were: ten cycles between 0% and 3% strain at 0.5 Hz, hold at 0% strain for 60 s, ramp to 5% strain at 15%/s and hold for 300 s, return to 0% strain and hold for 60 s, and lastly ramp at 1%/s until failure.

Actuator position and linear force were measured at a rate of approximately 10 Hz throughout the duration of the test, and stress was designated as the force divided by initial CSA. Peak stress, equilibrium stress, and percent relaxation were calculated from stress relaxation data. The time required to reach 50% of the total relaxation was determined and recorded as the relaxation time. Bilinear curve fitting using the least squares method was used to determine toe and linear region properties from the force-displacement and stress–strain curves of the ramp to failure, and the transition point was recorded at the intersection of the two best fit lines. Only the linear modulus was determined from samples which did not have a clear toe region of the stress–strain curve. Failure data were not reported because the mode of failure was not consistent across all samples.

Quantitative Polarized Light Imaging and Strain Tracking. A quantitative polarized light imaging (QPLI) system was used to capture video of the mechanical test. The system consisted of a light-emitting diode fiber optic light, a linear polarizing film and quarter wave retarder film, a 65 mm macrolens, and a division-of-focal-plane polarization camera [41]. Taking advantage of the natural birefringence of collagen, the QPLI system allowed the determination of the degree of linear polarization (DoLP) and the angle of polarization (AoP) of the light transmitted through the tendon in real time, which represent the overall strength and direction of collagen alignment, respectively [42,43].

Recorded video was analyzed using a custom MATLAB code. Briefly, for each frame being analyzed, a ROI within the tendon between the two Verhoeff's stain lines was located by binarizing the raw intensity image using intensity thresholds. The average (AVG) DoLP and the standard deviation (STD) of the AoP within the ROI were calculated as described previously (Fig. 1) [42,44,45]. Larger AVG DoLP values indicate more strongly aligned collagen fibers, while larger STD AoP values indicate less uniformly oriented fibers. Furthermore, the corners of the ROI were tracked throughout the ramp to failure and were used to determine the two-dimensional Lagrangian strain based on the least-squares solution of the deformation tensor and displacement vector [4].

Data Analysis. Two-way analysis of variance (ANOVA) tests were performed to determine the effects of genotype, tendon type, and their interaction on tendon composition, CSA, and mechanical properties. From the TEM images, the diameters of the first 1000 measured collagen fibrils from each sample were pooled together by group. Visual assessment of histograms of these data showed that collagen fibril diameter distributions were non-normal, so the Mann–Whitney test was used to determine differences in mean rank between genotypes. Comparisons of area fractions between genotypes were performed using unpaired two tailed *t*-tests.

Because the QPLI data are dependent on tissue thickness (which varied by tendon type), comparisons were not made between tendons; analyses of AVG DoLP and STD AoP were carried out separately for SSTs and ATs. Repeated-measures two-way ANOVAs were performed on QPLI data to determine the effect of genotype, time, and their interaction during stress relaxation, and to determine the effect of genotype, applied strain, and their interaction during ramp to failure. Where the sphericity assumption was not met (as determined by Mauchly's test), the Greenhouse–Geisser correction was applied to adjust the resultant *p*-values. As standard post hoc tests do not account for deviations from sphericity, multiple comparisons were not made on these data [46].

Statistical analyses were performed using SAS Studio 3.6, and plots were created using GraphPad Prism 7.03. In all cases, *p*-values less than 0.05 were considered significant and *p*-values between 0.05 and 0.10 were considered trending toward significance. Data are presented as mean ± standard deviation. Percent differences between genotypes or tendon types are reported as the

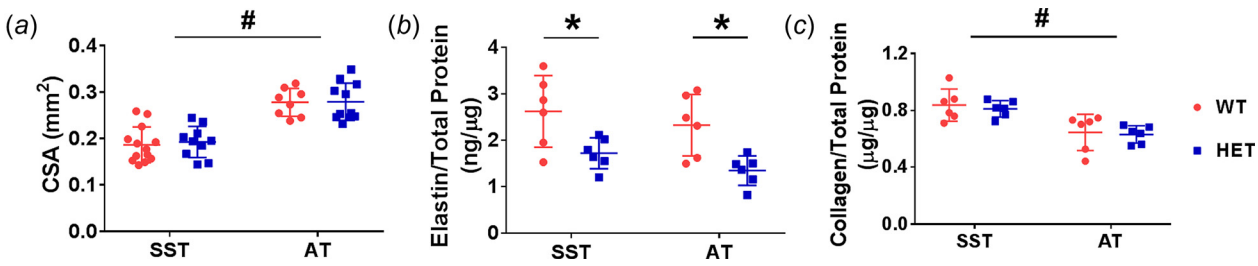

Fig. 2 CSA was greater in ATs than SSTs and was unaffected by genotype (*a*). Elastin content was decreased in HET tendons and was similar between tendon types (*b*). Collagen content was decreased in ATs and was unaffected by genotype (*c*). Two-way ANOVA *genotype effect $p < 0.05$; #tendon type effect $p < 0.05$.

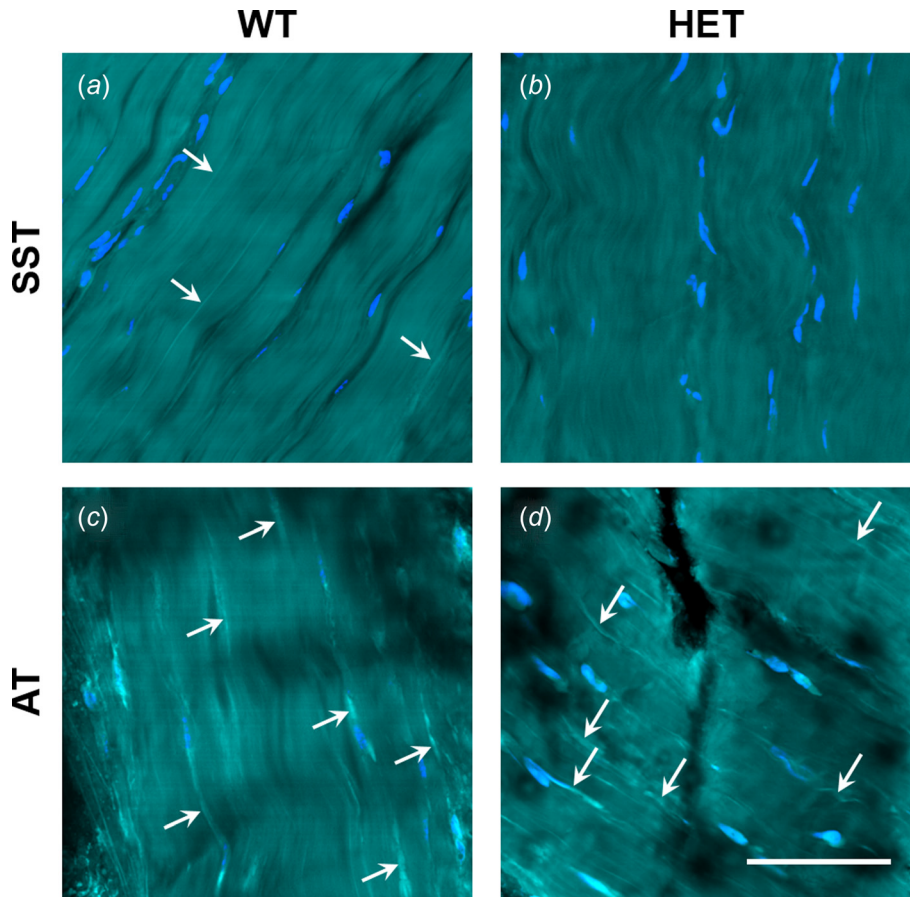

Fig. 3 Distribution of SRB-stained elastic fibers (bright cyan; white arrows), tenocytes (blue), and collagen (cyan) in WT and HET SSTs and ATs. Few or no fibers were visible in SSTs (*a*,*b*). Stained fibers are visible in WT and HET ATs (*c*,*d*), where they conformed to collagen orientation and were often localized near tenocytes. No differences were evident between genotypes. Scale bar = 50 μm. Refer to online version for color figure.

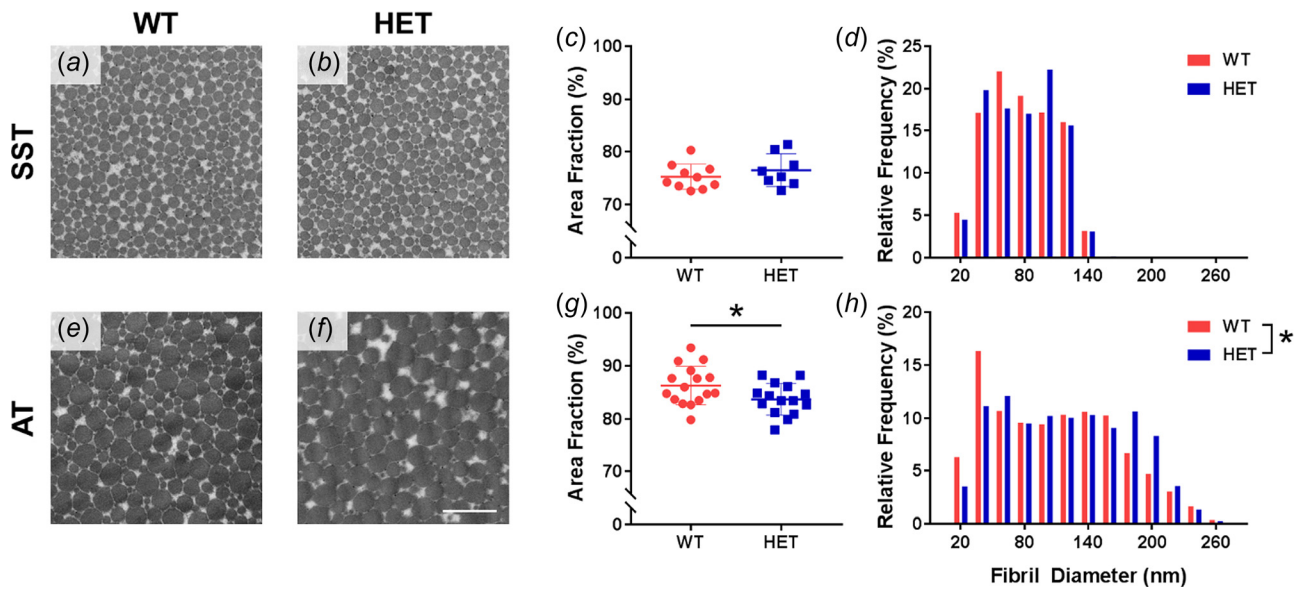

Fig. 4 Representative TEM micrographs from WT and HET SSTs and ATs (*a*,*b*,*e*,*f*). Scale bar = 500 nm. Elastin haploinsufficiency caused no change in SST collagen nanostructure (*c*,*d*), while HET ATs had decreased area fraction (*g*) and altered fibril diameter distribution (*h*). *Genotype effect $p < 0.05$.

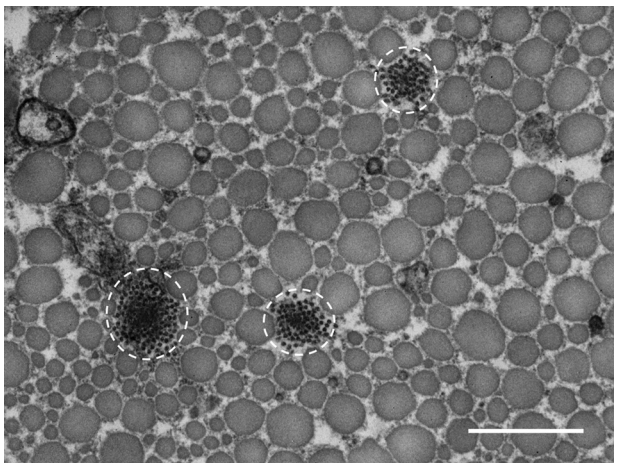

Fig. 5 Representative TEM micrograph from a HET SST showing groups of fibrillin microfibrils with varying amounts of elastin, circled in white. Scale bar = 500 nm.

difference between the least squares mean of the respective groups.

Results

Composition and Structure. There were no significant interactions between genotype and tendon type for CSA, elastin content, or collagen content. Tendon CSA was 48% larger in ATs than SSTs ($p < 0.001$) and was not affected by genotype (Fig. 2(*a*)). Elastin content was decreased in HET tendons by approximately 38% in SSTs and ATs ($p < 0.001$), and elastin quantity was not different between the two tendons (Fig. 2(*b*)). Average collagen content ranged between 63–84% and was not affected by genotype, but was 23% lower in ATs compared to SSTs ($p < 0.001$) (Fig. 2(*c*)).

Two-photon microscopy images showed an organized collagen network with tenocytes arranged in rows parallel to the collagen fibers for both tendons and genotypes (Fig. 3). In ATs, SRB-stained elastic fibers generally conformed to the collagen crimp pattern and were often localized around tenocytes. Very few elastic fibers were visible in SST images. There were no obvious qualitative differences in the number or distribution of SRB-stained elastic fibers between genotypes for either tendon.

Analysis of TEM micrographs showed that there was no difference in area fraction or fibril diameter distribution between WT and HET SSTs (Figs. 4(*a*)–4(*d*)). In contrast, there was a significant difference between the genotypes in both area fraction ($p = 0.039$) and fibril diameter distribution ($p < 0.001$) of the ATs (Figs. 4(*e*)–4(*h*)). Compared to WT tendons, HET tendons had a smaller collagen area fraction, fewer small (<50 nm) fibrils, and more large (>170 nm) fibrils. Furthermore, both elastic fibers and oxytalan fibers (fibrillin microfibrils without elastin) were visible in TEM images from all tendon groups (Fig. 5).

Stress Relaxation. There were no significant interactions between genotype and tendon type or any effect of genotype on any mechanical stress relaxation parameters. Achilles tendons had greater peak stress (81% increase), equilibrium stress (85% increase), and relaxation time (46% increase) than SSTs ($p < 0.001$), and percent relaxation was unaffected by tendon type (Table 1).

Changes in collagen alignment during stress relaxation are shown in Fig. 6. There were no significant interactions between the two factors (i.e., genotype and time) in AVG DoLP and STD AoP, and no effect of genotype on AVG DoLP for both tendons. In ATs, the HET tendons showed a trend toward decreased STD AoP ($p = 0.087$), yet genotype had no effect on STD AoP in

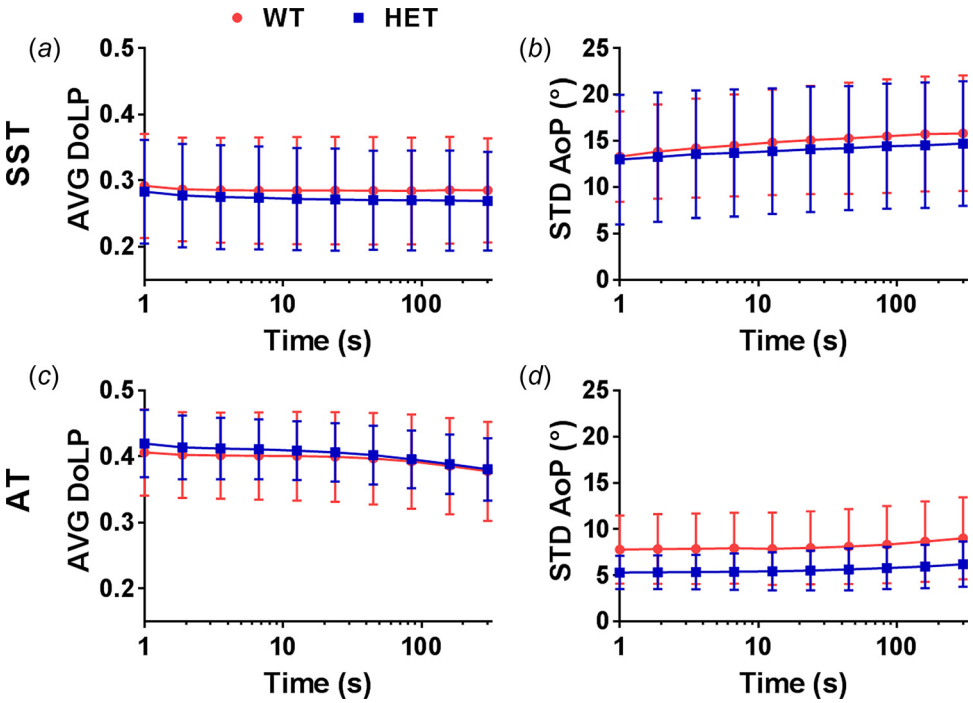

Fig. 6 Changes in collagen alignment during stress relaxation are represented by AVG DoLP and STD AoP. In both tendons, AVG DoLP decreased (*a,c*) and STD AoP increased (*b,d*) as time progressed. There was a trend toward decreased STD AoP in HET ATs compared to WT ATs. Note: The initial time of the test was set to 1 s to allow graphical representation on a logarithmic scale. AVG DoLP *y*-axes do not start at 0.

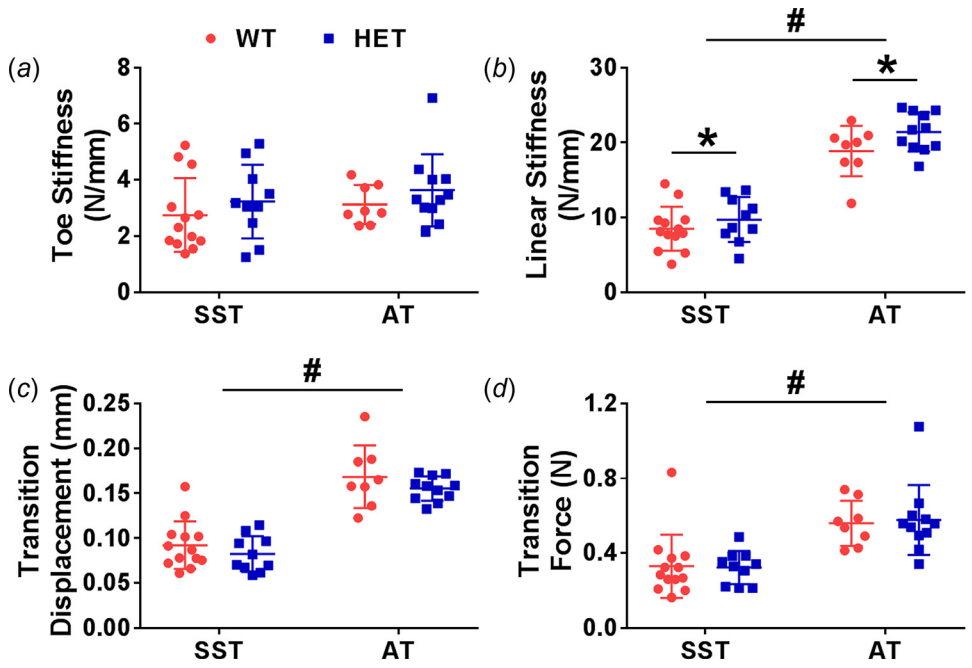

Fig. 7 Toe stiffness was similar across both genotypes and tendon types (*a*). Linear stiffness was greater in ATs and was increased in HET tendons (*b*). Transition displacement and transition force were greater in ATs and not affected by genotype (*c*,*d*). Two-way ANOVA *genotype effect $p < 0.05$; #tendon type effect $p < 0.05$.

SSTs. Moreover, AVG DoLP decreased ($p \leq 0.005$) and STD AoP increased ($p < 0.001$) as time progressed in both tendons, indicating a decrease in strength and uniformity of collagen alignment during the stress relaxation portion of the test protocol.

Ramp to Failure. There were no significant interactions between genotype and tendon type in any mechanical ramp to failure parameters. Tendons from HET mice had significantly increased linear stiffness compared to WT tendons by an average of 14% ($p = 0.049$). Toe stiffness, transition displacement, and transition force were unaffected by genotype. Linear stiffness (121% increase), transition displacement (86% increase), and transition force (74% increase) were greater in ATs than SSTs ($p < 0.001$), while toe stiffness was unaffected by tendon type (Fig. 7). Material properties were generally more variable than structural properties, and there was no effect of genotype on toe

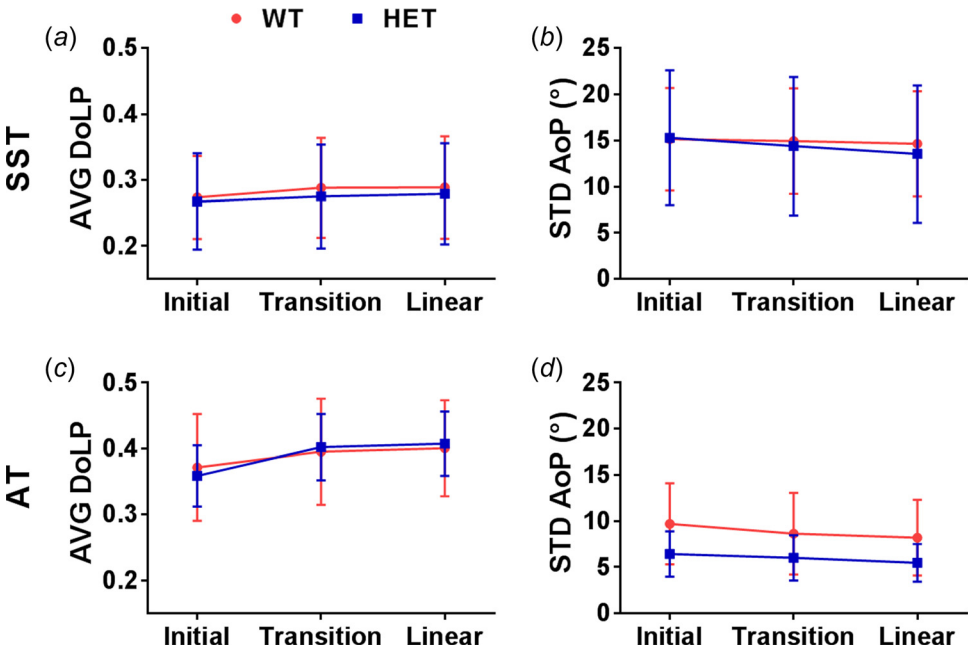

Fig. 8 Changes in collagen alignment during ramp to failure are represented by AVG DoLP and STD AoP. In both tendons, AVG DoLP increased (*a*,*c*) and STD AoP decreased (*b*,*d*) with increasing strain. There was a greater increase in AVG DoLP from initial to transition regions and a trend toward decreased STD AoP in HET ATs compared to WT ATs. Note: AVG DoLP *y*-axes do not start at 0.

Table 1 Mechanical properties of WT and HET SSTs and ATs. Elastin haploinsufficiency increased the linear stiffness of both tendons, and numerous differences between SSTs and ATs were detected.

	SST		AT	
Parameter	WT ($n = 13$)	HET ($n = 10$)	WT ($n = 8$)	HET ($n = 11$)
Peak stress (MPa)[#]	5.96 ± 3.23	6.69 ± 2.33	10.55 ± 2.97	12.31 ± 2.08
Equilibrium stress (MPa)[#]	3.92 ± 2.09	4.54 ± 1.74	7.20 ± 2.19	8.46 ± 1.62
Percent relaxation (%)	33.72 ± 6.85	32.72 ± 6.39	32.22 ± 3.35	31.43 ± 3.25
Relaxation time (s)[#]	2.38 ± 0.65	2.30 ± 0.73	3.40 ± 0.64	3.43 ± 0.72
Toe stiffness (N/mm)	2.75 ± 1.31	3.23 ± 1.31	3.13 ± 0.69	3.64 ± 1.28
Linear stiffness (N/mm)[*] [#]	8.50 ± 2.95	9.72 ± 2.98	18.86 ± 3.37	21.42 ± 2.62
Transition displacement (mm)[#]	0.092 ± 0.027	0.082 ± 0.020	0.168 ± 0.035	0.155 ± 0.014
Transition force (N)[#]	0.331 ± 0.168	0.323 ± 0.089	0.560 ± 0.120	0.577 ± 0.187
Toe modulus (MPa)[#]	27.15 ± 8.25	33.02 ± 30.63[a]	78.86 ± 59.54	48.36 ± 30.36[a]
Linear modulus (MPa)[#]	101.2 ± 50.8	129.4 ± 96.3	443.8 ± 131.7	485.3 ± 141.6
Transition strain (%)[#]	4.75 ± 3.00	4.19 ± 2.62[a]	1.54 ± 1.17	2.30 ± 1.57[a]
Transition stress (MPa)	1.68 ± 0.83	1.99 ± 1.83[a]	1.21 ± 0.83	1.07 ± 0.81[a]

[a] $n = 9$. Two-way ANOVA.
[*] genotype effect $p < 0.05$.
[#] tendon type effect $p < 0.05$. All interaction effects $p > 0.05$.

modulus, linear modulus, transition strain, or transition stress. Still, the toe modulus (111% increase) and linear modulus (303% increase) values were larger and the transition strain values were smaller (57% decrease) in ATs compared to SSTs ($p \leq 0.005$), while there was no effect of tendon type on transition stress (Table 1).

Polarization data were analyzed at the initial, transition (intersection of bilinear curve fitting), and linear (double the displacement at transition) regions of the ramp to failure (Fig. 8). In SSTs, there were no significant interactions between genotype and strain region and no effect of genotype on AVG DoLP and STD AoP. The collagen fibers became more strongly and uniformly aligned throughout the test, demonstrated by an increase in AVG DoLP ($p = 0.020$) and decrease in STD AoP ($p = 0.011$). In contrast to the SSTs, there was a significant interaction between genotype and strain region in AVG DoLP of the ATs ($p = 0.043$) due to the larger increase from the initial to transition regions in the HETs (12%) compared to the WTs (6%). Still, there was no difference in AVG DoLP values between genotypes. Similar to the results from stress relaxation, there was no significant interaction between genotype and strain region in STD AoP, and there was a trend toward decreased STD AoP values in HET tendons ($p = 0.074$). Additionally, STD AoP decreased throughout the test in ATs ($p < 0.001$).

Discussion

In agreement with changes in ascending aortae [35], tendons from the HET mice had significantly decreased quantitative levels of crosslinked elastin as determined by ELISA. In comparing the two tendon types, the images of SRB-stained tendons suggested a greater number of elastic fibers in ATs; however, the biochemical results did not show a difference in elastin content between tendon types. Because the ELISA only quantifies mature, fully crosslinked elastin, this may indicate a greater quantity of less mature elastic fibers in the AT. Furthermore, it is not clear whether SRB binds to elastin or fibrillins in elastic fibers, and therefore, the lack of an obvious qualitative difference in two-photon microscopy images between genotypes may be due to staining of elastin-free oxytalan fibers in HET tendons.

The mechanical properties of HET tendons remained largely unchanged despite the decreased elastin content, with a slight increase in linear stiffness being the only detectable mechanical effect of elastin haploinsufficiency. This stiffening effect is similar to what has been shown in the arteries of the same mouse model [29,31], and may result from more complete collagen engagement in HET tendons since there are fewer elastic fibers to resist structural reorganization [47]. This is further evidenced in ATs by the larger increase in AVG DoLP during ramp to failure and potentially the trend toward lower STD AoP, which together indicate that HET ATs may have more uniformly oriented collagen fibers that become aligned more quickly upon loading, leading to a slightly stiffer response. While these results on collagen alignment agree with our hypothesis of a greater effect of elastin haploinsufficiency in ATs, it did not manifest into any tendon specific changes in mechanical properties. Indeed, neither SSTs nor ATs experienced any major mechanical impairment from the elastin deficiency.

The lack of a mechanical difference here is in contrast to studies that reported significant changes upon elastase treatment of human palmaris longus tendons [48], human SSTs [25], and bovine medial collateral ligaments [26,27]. Collectively, these studies report decreased resistance to off-axis loading and low-strain tensile loading, with a slightly decreased or unchanged linear modulus in elastase treated samples. It may be that potential off-target effects of elastase, such as digestion of glycosaminoglycans or collagen [24,26], contributed to the change in mechanics. However, glycosaminoglycan depletion does not have a large effect on connective tissue mechanics [49–51] and a minor disruption of collagen is unlikely to account for the large effects reported in these studies. Alternatively, there may be a species-specific effect of elastic fibers related to the size of the tendons. Since murine tendons are much smaller than the samples listed above, they may contain less or no IFM space and correspondingly fewer elastic fibers in comparison to tendons from larger mammals. Supporting this concept, our measured elastin content is a level of magnitude smaller than that in human SSTs [25]. Additionally, elastase treated rat tail tendon fascicles (similar in size to mouse SSTs and ATs) do not exhibit any change in prefailure mechanical properties [24,48]. Consequently, elastic fibers may play an important role in strain attenuation of larger tendons but are less significant in smaller tendons.

Furthermore, developmental compensation is common in genetically modified animals. Indeed, the HET mice develop arteries with an increased number of elastic lamellae and a smaller diameter to maintain normal blood flow in spite of chronic hypertension [29,52], and also maintain normal pulmonary structure under unstressed conditions [53]. Although the CSA and total collagen content were similar between HET and WT tendons, the decreased collagen area fraction and altered fibril diameter distribution in ATs determined from TEM micrographs may be a compensatory mechanism to maintain normal tendon function with decreased elastin. This tendon-specific change in collagen structure may explain why the change in AT mechanical properties

was not greater than the change in SSTs. Moreover, there are a number of other possible compensatory mechanisms which were not investigated here. For example, similar to elastic fibers, lubricin resides primarily in the IFM of tendons and facilitates sliding between fascicles [54–56]. Moreover, crosslinking of collagen and elastin are both mediated by the enzyme lysyl oxidase [57], and therefore, HET tendons may have altered collagen crosslinking which has been shown to influence mechanical properties [58–60].

In addition to the AT-specific changes in collagen structure and alignment from elastin haploinsufficiency, it is worth briefly reviewing the mechanical differences between the SST and AT. While studies using digital flexor and extensor tendons report a higher linear modulus in positional tendons [61,62], the SST is unique among positional tendons due to complex multiaxial loading in vivo, and therefore, the results may not be directly comparable. Previous reports are mixed on mechanical differences between murine SSTs and ATs [63,64], yet our data showed that ATs are stronger and take more time to relax than SSTs, which is consistent with a previous report of tendons containing larger fibrils exhibiting a greater linear modulus [61]. Further work into tendon specific differences may incorporate a more standard positional tendon, such as the tibialis anterior tendon, along with the SST and AT to determine the conservation of mechanical differences of functionally distinct tendons across species.

Although we did not find any major changes to the mechanical properties or collagen alignment in HET tendons, this work only investigated tissue from young, healthy mice. It is conceivable that the effect of elastin haploinsufficiency may become greater with advanced age or with a controlled exercise routine, potentially leading to overuse injuries. In addition, thorough study of the compensatory effects in developing HET mice may provide insight in to the role of elastic fibers in tendon development. Finally, evaluation of other mouse models with altered elastic fibers ($Fbn1^{+/-}$, $Fbln5^{-/-}$) could improve understanding of the contributions of the specific components of elastic fibers. Thus, continued research is necessary to more fully comprehend how elastic fibers contribute to tendon function in health, in disease or injury, and in development and aging.

To conclude, elastin haploinsufficiency caused an increase in tendon stiffness in both tendon types and structural changes only in the AT. The results presented here demonstrate a minor yet statistically significant impact of elastic fibers on structure–function relationships in tendon which differs between functionally distinct tendons.

Acknowledgment

We thank Robyn Roth for her contribution to TEM sample preparation and Lauren Zhou for her contribution to TEM image analysis.

Funding Data

- Division of Civil, Mechanical and Manufacturing Innovation, National Science Foundation (NSF) (Grant No. CMMI 1562107).

References

[1] Kannus, P., 2000, "Structure of the Tendon Connective Tissue," Scand. J. Med. Sci. Sports, **10**(6), pp. 312–320.
[2] Screen, H. R. C., Berk, D. E., Kadler, K. E., Ramirez, F., and Young, M. F., 2015, "Tendon Functional Extracellular Matrix," J. Orthop. Res., **33**(6), pp. 793–799.
[3] Thorpe, C. T., Klemt, C., Riley, G. P., Birch, H. L., Clegg, P. D., and Screen, H. R. C., 2013, "Helical Sub-Structures in Energy-Storing Tendons Provide a Possible Mechanism for Efficient Energy Storage and Return," Acta Biomater., **9**(8), pp. 7948–7956.
[4] Fang, F., and Lake, S. P., 2015, "Multiscale Strain Analysis of Tendon Subjected to Shear and Compression Demonstrates Strain Attenuation, Fiber Sliding, and Reorganization," J. Orthop. Res., **33**(11), pp. 1704–1712.
[5] Fang, F., and Lake, S. P., 2017, "Experimental Evaluation of Multiscale Tendon Mechanics," J. Orthop. Res., **35**(7), pp. 1353–1365.
[6] Hansen, K. A., Weiss, J. A., and Barton, J. K., 2002, "Recruitment of Tendon Crimp With Applied Tensile Strain," ASME J. Biomech. Eng., **124**(1), pp. 72–77.
[7] Miller, K. S., Connizzo, B. K., Feeney, E., and Soslowsky, L. J., 2012, "Characterizing Local Collagen Fiber Re-Alignment and Crimp Behavior Throughout Mechanical Testing in a Mature Mouse Supraspinatus Tendon Model," J. Biomech., **45**(12), pp. 2061–2065.
[8] Lake, S. P., Miller, K. S., Elliott, D. M., and Soslowsky, L. J., 2009, "Effect of Fiber Distribution and Realignment on the Nonlinear and Inhomogeneous Mechanical Properties of Human Supraspinatus Tendon Under Longitudinal Tensile Loading," J. Orthop. Res., **27**(12), pp. 1596–1602.
[9] Thorpe, C. T., Birch, H. L., Clegg, P. D., and Screen, H. R. C., 2013, "The Role of the Non-Collagenous Matrix in Tendon Function," Int. J. Exp. Pathol., **94**(4), pp. 248–259.
[10] Baldwin, A. K., Simpson, A., Steer, R., Cain, S. A., and Kielty, C. M., 2013, "Elastic Fibres in Health and Disease," Expert Rev. Mol. Med., **15**(e8), pp. 1–30.
[11] Montes, G., 1996, "Structural Biology of the Fibres of the Collagenous and Elastic Systems," Cell Biol. Int., **20**(1), pp. 15–27.
[12] Sherratt, M. J., 2009, "Tissue Elasticity and the Ageing Elastic Fibre," Age (Omaha), **31**(4), pp. 305–325.
[13] Kostrominova, T. Y., and Brooks, S. V., 2013, "Age-Related Changes in Structure and Extracellular Matrix Protein Expression Levels in Rat Tendons," Age (Omaha), **35**(6), pp. 2203–2214.
[14] Thorpe, C. T., Riley, G. P., Birch, H. L., Clegg, P. D., and Screen, H. R. C., 2017, "Fascicles and the Interfascicular Matrix Show Adaptation for Fatigue Resistance in Energy Storing Tendons," Acta Biomater., **42**, pp. 308–315.
[15] Sugitani, H., Hirano, E., Knutsen, R. H., Shifren, A., Wagenseil, J. E., Ciliberto, C., Kozel, B. A., Urban, Z., Davis, E. C., Broekelmann, T. J., and Mecham, R. P., 2012, "Alternative Splicing and Tissue-Specific Elastin Misassembly Act as Biological Modifiers of Human Elastin Gene Frameshift Mutations Associated With Dominant Cutis Laxa," J. Biol. Chem., **287**(26), pp. 22055–22067.
[16] Zeyer, K. A., and Reinhardt, D. P., 2015, "Engineered Mutations in Fibrillin-1 Leading to Marfan Syndrome Act at the Protein, Cellular and Organismal Levels," Mutat. Res. Rev. Mutat. Res., **765**, pp. 7–18.
[17] Wu, Y. T., Wu, P. T., and Jou, I. M., 2016, "Peritendinous Elastase Treatment Induces Tendon Degeneration in Rats: A Potential Model of Tendinopathy In Vivo," J. Orthop. Res., **34**(3), pp. 471–477.
[18] Wu, Y.-T., Su, W.-R., Wu, P.-T., Shen, P.-C., and Jou, I.-M., 2017, "Degradation of Elastic Fiber and Elevated Elastase Expression in Long Head of Biceps Tendinopathy," J. Orthop. Res., **35**(9), pp. 1919–1926.
[19] Thakkar, D., Grant, T. M., Hakimi, O., and Carr, A. J., 2014, "Distribution and Expression of Type VI Collagen and Elastic Fibers in Human Rotator Cuff Tendon Tears," Connect. Tissue Res., **55**(5–6), pp. 397–402.
[20] Gosline, J., Lillie, M., Carrington, E., Guerette, P., Ortlepp, C., and Savage, K., 2002, "Elastic Proteins: Biological Roles and Mechanical Properties," Philos. Trans. R. Soc. B Biol. Sci., **357**(1418), pp. 121–132.
[21] Baldock, C., Oberhauser, A. F., Ma, L., Lammie, D., Siegler, V., Mithieux, S. M., Tu, Y., Chow, J. Y. H., Suleman, F., Malfois, M., Rogers, S., Guo, L., Irving, T. C., Wess, T. J., and Weiss, A. S., 2011, "Shape of Tropoelastin, the Highly Extensible Protein That Controls Human Tissue Elasticity," Proc. Natl. Acad. Sci. U. S. A., **108**(11), pp. 4322–4327.
[22] Grant, T. M., Thompson, M. S., Urban, J., and Yu, J., 2013, "Elastic Fibres Are Broadly Distributed in Tendon and Highly Localized Around Tenocytes," J. Anat., **222**(6), pp. 573–579.
[23] Pang, X., Wu, J.-P., Allison, G. T., Xu, J., Rubenson, J., Zheng, M.-H., Lloyd, D. G., Gardiner, B., Wang, A., and Kirk, T. B., 2017, "Three Dimensional Microstructural Network of Elastin, Collagen, and Cells in Achilles Tendons," J. Orthop. Res., **35**(6), pp. 1203–1214.
[24] Grant, T. M., Yapp, C., Chen, Q., Czernuszka, J. T., and Thompson, M. S., 2015, "The Mechanical, Structural, and Compositional Changes of Tendon Exposed to Elastase," Ann. Biomed. Eng., **43**(10), pp. 2477–2486.
[25] Fang, F., and Lake, S. P., 2016, "Multiscale Mechanical Integrity of Human Supraspinatus Tendon in Shear After Elastin Depletion," J. Mech. Behav. Biomed. Mater., **63**, pp. 443–455.
[26] Henninger, H. B., Valdez, W. R., Scott, S. A., and Weiss, J. A., 2015, "Elastin Governs the Mechanical Response of Medial Collateral Ligament Under Shear and Transverse Tensile Loading," Acta Biomater., **25**, pp. 304–312.
[27] Henninger, H. B., Underwood, C. J., Romney, S. J., Davis, G. L., and Weiss, J. A., 2013, "Effect of Elastin Digestion on the Quasi-Static Tensile Response of Medial Collateral Ligament," J. Orthop. Res., **31**(8), pp. 1226–1233.
[28] Li, D. Y., Brooke, B., Davis, E. C., Mecham, R. P., Sorensen, L. K., Boak, B. B., Eichwald, E., and Keating, M. T., 1998, "Elastin is an Essential Determinant of Arterial Morphogenesis," Nature, **393**(6682), pp. 276–280.
[29] Li, D. Y., Faury, G., Taylor, D. G., Davis, E. C., Boyle, W. A., Mecham, R. P., Stenzel, P., Boak, B., and Keating, M. T., 1998, "Novel Arterial Pathology in Mice and Humans Hemizygous for Elastin," J. Clin. Invest., **102**(10), pp. 1783–1787.
[30] Wagenseil, J. E., Nerurkar, N. L., Knutsen, R. H., Okamoto, R. J., Li, D. Y., Mecham, R. P. E. J., Knut-, R. H., and Effects, R. P. M., 2005, "Effects of Elastin Haploinsufficiency on the Mechanical Behavior of Mouse Arteries," Am. J. Physiol. Hear. Circ. Physiol, **289**(3), pp. H1209–H1217.
[31] Carta, L., Wagenseil, J. E., Knutsen, R. H., Mariko, B., Faury, G., Davis, E. C., Starcher, B., Mecham, R. P., and Ramirez, F., 2009, "Discrete Contributions of Elastic Fiber Components to Arterial Development and Mechanical Compliance," Arterioscler. Thromb. Vasc. Biol., **29**(12), pp. 2083–2089.

[32] Thorpe, C. T., Karunaseelan, K. J., Ng Chieng Hin, J., Riley, G. P., Birch, H. L., Clegg, P. D., and Screen, H. R. C., 2016, "Distribution of Proteins Within Different Compartments of Tendon Varies According to Tendon Type," J. Anat., **229**(3), pp. 450–458.
[33] Thorpe, C. T., Godinho, M. S. C., Riley, G. P., Birch, H. L., Clegg, P. D., and Screen, H. R. C., 2015, "The Interfascicular Matrix Enables Fascicle Sliding and Recovery in Tendon, and Behaves More Elastically in Energy Storing Tendons," J. Mech. Behav. Biomed. Mater., **52**, pp. 85–94.
[34] Alexander, R. M., 1991, "Energy-Saving Mechanisms in Walking and Running," J. Exp. Biol., **160**, pp. 55–69.
[35] Cheng, J. K., Stoilov, I., Mecham, R. P., and Wagenseil, J. E., 2013, "A Fiber-Based Constitutive Model Predicts Changes in Amount and Organization of Matrix Proteins With Development and Disease in the Mouse Aorta," Biomech. Model. Mechanobiol., **12**(3), pp. 497–510.
[36] Jamall, I. S., Finelli, V. N., and Que Hee, S. S., 1981, "A Simple Method to Determine Nanogram Levels of 4-Hydroxyproline in Biological Tissues," Anal. Biochem., **112**(1), pp. 70–75.
[37] Neuman, R. E., and Logan, M. A., 1950, "The Determination of Hydroxyproline," J. Biol. Chem., **184**(1), pp. 299–306.
[38] Starcher, B., 2001, "A Ninhydrin-Based Assay to Quantitate the Total Protein Content of Tissue Samples," Anal. Biochem., **292**(1), pp. 125–129.
[39] Ricard, C., Vial, J.-C., Douady, J., and van der Sanden, B., 2015, "In Vivo Imaging of Elastic Fibers Using Sulforhodamine B," J. Biomed. Opt., **12**(6), p. 064017.
[40] Starborg, T., Kalson, N. S., Lu, Y., Mironov, A., Cootes, T. F., Holmes, D. F., and Kadler, K. E., 2013, "Using Transmission Electron Microscopy and 3View to Determine Collagen Fibril Size and Three-Dimensional Organization," Nat. Protoc., **8**(7), pp. 1433–1448.
[41] York, T., and Gruev, V., 2012, "Characterization of a Visible Spectrum Division-of-Focal-Plane Polarimeter," Appl. Opt., **51**(22), pp. 5392–5400.
[42] York, T., Kahan, L., Lake, S. P., and Gruev, V., 2014, "Real-Time High-Resolution Measurement of Collagen Alignment in Dynamically Loaded Soft Tissue," J. Biomed. Opt., **19**(6), p. 66011.
[43] York, T., Powell, S. B., Gao, S., Kahan, L., Charanya, T., Saha, D., Roberts, N. W., Cronin, T. W., Marshall, J., Achilefu, S., Lake, S. P., Raman, B., and Gruev, V., 2014, "Bioinspired Polarization Imaging Sensors: From Circuits and Optics to Signal Processing Algorithms and Biomedical Applications," Proc. IEEE. Inst. Electr. Electron. Eng., **102**(10), pp. 1450–1469.
[44] Skelley, N. W., Castile, R. M., York, T. E., Gruev, V., Lake, S. P., and Brophy, R. H., 2015, "Differences in the Microstructural Properties of the Anteromedial and Posterolateral Bundles of the Anterior Cruciate Ligament," Am. J. Sports Med., **43**(4), pp. 928–936.
[45] Castile, R. M., Skelley, N. W., Babaei, B., Brophy, R. H., and Lake, S. P., 2016, "Microstructural Properties and Mechanics Vary Between Bundles of the Human Anterior Cruciate Ligament During Stress-Relaxation," J. Biomech., **49**(1), pp. 87–93.
[46] Armstrong, R. A., 2017, "Statistical Review: Recommendations for Analysis of Repeated-Measures Designs: Testing and Correcting for Sphericity and Use of Manova and Mixed Model Analysis," Ophthalmic Physiol. Opt., **37**(5), pp. 585–593.
[47] Lake, S. P., and Barocas, V. H., 2011, "Mechanical and Structural Contribution of Non-Fibrillar Matrix in Uniaxial Tension: A Collagen-Agarose Co-Gel Model," Ann. Biomed. Eng., **39**(7), pp. 1891–1903.
[48] Millesi, H., Reihsner, R., Hamilton, G., Mallinger, R., and Menzel, E. J., 1995, "Biomechanical Properties of Normal Tendons, Normal Palmar Aponeuroses, and Tissues From Patients With Dupuytren's Disease Subjected to Elastase and Chondroitinase Treatment," Clin. Biomech., **10**(1), pp. 29–35.
[49] Fang, F., and Lake, S. P., 2017, "Multiscale Mechanical Evaluation of Human Supraspinatus Tendon Under Shear Loading After Glycosaminoglycan Reduction," ASME J. Biomech. Eng., **139**(7), p. 071013.
[50] Fessel, G., and Snedeker, J. G., 2011, "Equivalent Stiffness After Glycosaminoglycan Depletion in Tendon—An Ultra-Structural Finite Element Model and Corresponding Experiments," J. Theor. Biol., **268**(1), pp. 77–83.
[51] Lujan, T. J., Underwood, C. J., Henninger, H. B., Thompson, B. M., and Weiss, J. A., 2007, "Effect of Dermatan Sulfate Glycosaminoglycans on the Quasi-Static Material Properties of the Human Medial Collateral Ligament," J. Orthop. Res., **25**(7), pp. 894–903.
[52] Faury, G., Pezet, M., Knutsen, R. H., Boyle, W. A., Heximer, S. P., McLean, S. E., Minkes, R. K., Blumer, K. J., Kovacs, A., Kelly, D. P., Li, D. Y., Starcher, B., and Mecham, R. P., 2003, "Developmental Adaptation of the Mouse Cardiovascular System to Elastin Haploinsufficiency," J. Clin. Invest., **112**(9), pp. 1419–1428.
[53] Shifren, A., Durmowicz, A. G., Knutsen, R. H., Hirano, E., and Mecham, R. P., 2006, "Elastin Protein Levels Are a Vital Modifier Affecting Normal Lung Development and Susceptibility to Emphysema," AJP Lung Cell. Mol. Physiol., **292**(3), pp. L778–L787.
[54] Hayashi, M., Zhao, C., Thoreson, A. R., Chikenji, T., Jay, G. D., An, K. N., and Amadio, P. C., 2013, "The Effect of Lubricin on the Gliding Resistance of Mouse Intrasynovial Tendon," PLoS One, **8**(12), p. e83836.
[55] Kohrs, R. T., Zhao, C., Sun, Y. L., Jay, G. D., Zhang, L., Warman, M. L., An, K. N., and Amadio, P. C., 2011, "Tendon Fascicle Gliding in Wild Type, Heterozygous, and Lubricin Knockout Mice," J. Orthop. Res., **29**(3), pp. 384–389.
[56] Sun, Y. L., Wei, Z., Zhao, C., Jay, G. D., Schmid, T. M., Amadio, P. C., and An, K. N., 2015, "Lubricin in Human Achilles Tendon: The Evidence of Intratendinous Sliding Motion and Shear Force in Achilles Tendon," J. Orthop. Res., **33**(6), pp. 932–937.
[57] Eyre, D. R., Paz, M. A., and Gallop, P. M., 1984, "Cross-Linking in Collagen and Elastin," Ann. Rev. Biochem, **53**(1), pp. 717–748.
[58] Makris, E. A., Responte, D. J., Paschos, N. K., Hu, J. C., and Athanasiou, K. A., 2014, "Developing Functional Musculoskeletal Tissues Through Hypoxia and Lysyl Oxidase-Induced Collagen Cross-Linking," Proc. Natl. Acad. Sci. U. S. A., **111**(45), pp. E4832–E4841.
[59] Eleswarapu, S. V., Responte, D. J., and Athanasiou, K. A., 2011, "Tensile Properties, Collagen Content, and Crosslinks in Connective Tissues of the Immature Knee Joint," PLoS One, **6**(10), p. e26178.
[60] Thorpe, C. T., Stark, R. J. F., Goodship, A. E., and Birch, H. L., 2010, "Mechanical Properties of the Equine Superficial Digital Flexor Tendon Relate to Specific Collagen Cross-Link Levels," Equine Vet. J., **42**(s38), pp. 538–543.
[61] Birch, H. L., 2007, "Tendon Matrix Composition and Turnover in Relation to Functional Requirements," Int. J. Exp. Pathol., **88**(4), pp. 241–248.
[62] Thorpe, C. T., Udeze, C. P., Birch, H. L., Clegg, P. D., and Screen, H. R. C., 2012, "Specialization of Tendon Mechanical Properties Results From Interfascicular Differences," J. R. Soc. Interface, **9**(76), pp. 3108–3117.
[63] Connizzo, B. K., Freedman, B. R., Fried, J. H., Sun, M., Birk, D. E., and Soslowsky, L. J., 2015, "Regulatory Role of Collagen V in Establishing Mechanical Properties of Tendons and Ligaments Is Tissue Dependent," J. Orthop. Res., **33**(6), pp. 882–888.
[64] Connizzo, B. K., Bhatt, P. R., Liechty, K. W., and Soslowsky, L. J., 2014, "Diabetes Alters Mechanical Properties and Collagen Fiber Re-Alignment in Multiple Mouse Tendons," Ann. Biomed. Eng., **42**(9), pp. 1880–1888.